

## Carbon loss and optical property changes during long-term photochemical and biological degradation of estuarine dissolved organic matter

Mary Ann Moran and Wade M. Sheldon, Jr.

Department of Marine Sciences, University of Georgia, Athens, Georgia 30602-3636

Richard G. Zepp

Ecosystems Research Division, National Exposure Research Laboratory, U.S. Environmental Protection Agency, Athens, Georgia 30605-2700

### Abstract

Terrestrially derived dissolved organic matter (DOM) impacts the optical properties of coastal seawater and affects carbon cycling on a global scale. We studied sequential long-term photochemical and biological degradation of estuarine dissolved organic matter from the Satilla River, an estuary in the southeastern United States that is dominated by vascular plant-derived organic matter. During photodegradation, dissolved organic carbon (DOC) loss (amounting to 31% of the initial DOC) was much less extensive than colored dissolved organic matter (CDOM) or fluorescent dissolved organic matter (FDOM) loss (50% and 56% of the initial CDOM and FDOM), and analysis of kinetics suggested a reservoir of DOC that was resistant to photodegradation. In contrast, CDOM photodegradation closely followed first-order kinetics over two half-lives with no indication of a nondegradable component. FDOM loss was slightly biased toward fluorophores considered representative of terrestrial humic substances. Additional changes in optical properties included increases in spectral slope and shifts in fluorescence excitation/emission maxima that were generally consistent with previous observations from field studies of photobleached DOM. Biological degradation of photobleached DOM was more rapid than that of unbleached material, and this net positive effect was evident even for extensively photodegraded material. Bacterial degradation caused shifts in the opposite direction from photochemical degradation for both spectral slope and excitation/emission maxima and thus dampened but did not eliminate changes in optical properties caused by photobleaching.

Photochemical processes that induce changes in natural dissolved organic matter (DOM) can influence many aspects of carbon cycling in marine environments. The sunlight-mediated conversion of DOM into inorganic forms (dissolved inorganic carbon, carbon monoxide) and into bacterial substrates (low-molecular-weight carbonyl compounds and others) increases turnover rates of DOM in surface waters (Bushaw et al. 1996; Miller and Moran 1997; Moran and Zepp 1997). The loss of color (i.e., photobleaching) that accompanies photochemical modification of DOM affects the optical properties of seawater and influences penetration of ultraviolet and photosynthetically active wavelengths (Vodacek et al. 1997). Changes in light penetration depth subsequently affect exposure of marine microorganisms to sunlight and can modify the activities of autotrophs and heterotrophs in both positive and negative ways (Herndl et al. 1997; Jeffrey et al. 1999; Moran and Zepp 2000). Photoreactions of DOM therefore play key roles in oceanic carbon cycling, potentially controlling the degradation of terrestrially derived DOM in estuaries and shallow continental shelf systems (Miller and Moran 1997; Vodacek et al. 1997) and driving the turnover of marine-derived DOM in the surface ocean (Opsahl and Benner 1998; Cherrier et al. 1999).

Several models have been used to predict the effects of

photodegradation on DOM cycling in coastal and open ocean environments (Mopper et al. 1991; Miller and Zepp 1995; Amon and Benner 1996; Moran and Zepp 1997). One of the most critical aspects of these quantitative models is the use of short-term data to predict long-term effects of photochemistry on DOM pools. Current models must extrapolate photodegradation kinetics to longer time frames (i.e., years) and, in the absence of appropriate data, assume that all components of the DOM pool are equally photochemically reactive.

A limited number of recent experimental studies have begun to address long-term photodegradation processes (Vodacek et al. 1997; Opsahl and Benner 1998). These studies show that DOM photodegradation operates over month-long or greater time scales in seawater. More information is needed, however, and few studies of short- or long-term duration have successfully disentangled photochemically mediated effects on the DOM pool from the biologically driven processes that simultaneously affect turnover and may interact with the direct photochemical processes (Miller and Moran 1997).

This study addresses the effects of long-term exposure to sunlight on turnover of estuarine DOM and examines changes in biological lability and optical properties that co-occur with photodegradation. DOM from the Satilla Estuary in the southeastern United States served as a model for vascular plant-derived terrestrial DOM that is exported to the coastal ocean.

### Acknowledgments

We thank L. R. Pomeroy for use of his equipment and two anonymous reviewers for helpful comments on this manuscript.

Support for this project was provided by the Office of Naval Research (N00014-98-1-0530 and N00014-98-F-0202).

### Materials and Methods

*DOM source and preparation*—Water was collected in August 1997 from the freshwater region of the Satilla Es-

Table 1. Changes in optical properties and dissolved organic carbon (DOC) concentration during photobleaching. Initial DOC concentration was 2046  $\mu\text{M C}$  (primary experiment) and 1972  $\mu\text{M C}$  (replication experiment). Changes ( $\Delta$ ) are expressed relative to the nonincubated control. Spectral slope coefficient ( $S$ ) is calculated from the nonlinear regression of absorptivity vs. wavelength from 290 nm to 400 nm. The specific absorption coefficient ( $a_{450}^*$ ) is calculated as  $a_{450}$  (predicted from the non-linear regression) divided by the DOC concentration (in  $\text{mg C L}^{-1}$ ).

Experiment/treatment	Light exposure (d)	$\Delta a_{350}$ (%)	$\Delta a_{450}$ (%)	$S$	$a_{450}^*$	$\Delta\text{DOC}$ ( $\mu\text{M}$ )	$\Delta\text{DOC}$ (%)
Primary experiment							
Control (incubated)	0	-4.0	-7.2	0.0142	0.766	73 $\pm$ 26	-3.6
16% photobleached	6	-15.9	-9.6	0.0143	0.715	193 $\pm$ 20	-9.4
25% photobleached	14	-25.1	-16.7	0.0144	0.675	314 $\pm$ 22	-15.3
44% photobleached	34	-44.2	-33.6	0.0151	0.524	486 $\pm$ 23	-23.8
64% photobleached	70	-63.8	-50.4	0.0153	0.367	628 $\pm$ 30	-30.7
Secondary experiment							
Control (incubated)	0	-2.0	+0.6	0.0146	0.537	66 $\pm$ 59	-3.3
12% photobleached	0.1	-12.3	-3.4	0.0144	0.532	226 $\pm$ 48	-11.4
21% photobleached	0.3	-20.5	-9.4	0.0146	0.516	388 $\pm$ 42	-19.7
32% photobleached	0.6	-31.5	-18.0	0.0144	0.480	457 $\pm$ 43	-23.2
59% photobleached	1.6	-59.1	-53.3	0.0155	0.310	706 $\pm$ 45	-35.8

tuary in coastal Georgia. The sample was sequentially filtered through ashed Whatman GF/F and deionized water-rinsed 0.2- $\mu\text{m}$  pore size polycarbonate filters. The initial concentration of dissolved organic carbon (DOC) was 2,046  $\mu\text{M C}$ .

**Photobleaching protocol**—Samples were irradiated inside a temperature-controlled environmental chamber using 120-cm 40-W BL350 fluorescent black-light tubes (mounted 12 cm from the samples; Industrial, Atlanta Light Bulbs) and a canopy of 240-cm 215-W and 120-cm 120-W cool-white fluorescent tubes (24 cm from the samples). Ultraviolet (UV) light intensity at the sample surface was 9.2  $\text{W m}^{-2}$  (9.0  $\text{W m}^{-2}$  UVA [315–400 nm] and 0.2  $\text{W m}^{-2}$  UVB [280–315 nm]), approximately 31% (UVA) and 25% (UVB) of the daily average UV summertime spectral irradiance at 30°N latitude. PAR intensity was 50  $\text{W m}^{-2}$ , approximately 13% of the daily average summertime spectral irradiance at 30°N. Irradiance was uniform throughout the area used for sample exposure.

The filter-sterilized estuarine water was irradiated in ashed quartz flasks containing 2 liters of sample. Flasks were placed under the light source in a recirculating water bath that maintained temperature at 7°C when the lights were on. Sterile magnetic stir bars were used to stir each flask continuously, and flasks were capped with sterile foam plugs. Because preliminary experiments showed measurable regrowth of bacteria in filter-sterilized water samples after 2 weeks, samples were refiltered at regular intervals. Every 5–7 d, samples were removed from the light source and filtered through exhaustively rinsed 0.2- $\mu\text{m}$  pore size polycarbonate filters to eliminate bacterial regrowth.

The samples were irradiated until 16, 25, 44, or 64% of the original absorptivity at 350 nm ( $a_{350}$ ) was lost; length of light exposure varied from 6 d (16% photobleached) to 70 d (64% photobleached). When target bleaching levels were reached, the flasks were covered in aluminum foil and left

inside the water bath. Two additional dark control treatments were also established. An incubated dark control was wrapped in aluminum foil at the start of the experiment, incubated inside the water bath, and filter-sterilized at 5–7-d intervals as described above. A nonincubated dark control was kept refrigerated (at 4°C) in the dark for the duration of the irradiation phase of the experiment; this treatment was not repeatedly filter sterilized and served as a control for effects of filtration and incubation in the water bath. At the end of the irradiation phase, samples were taken from all flasks and stored in the dark at 4°C for subsequent determination of DOC concentration and measurement of optical properties (*see below*). The remaining water was used in bacterial biodegradation assays.

**Biodegradation protocol**—Water from the four irradiated treatments and the two dark controls was filtered through 0.2- $\mu\text{m}$  pore size polycarbonate filters, amended with an inorganic nutrient solution (equivalent to 0.1% of sample volume) to eliminate N and P limitation (5  $\mu\text{M NH}_3$ , 5  $\mu\text{M NO}_3$ , and 1  $\mu\text{M PO}_4$ , final concentration), and inoculated with a natural bacterial inoculum (equivalent to 1% of sample volume) prepared by concentrating bacteria from the Sattilla Estuary over a 0.2- $\mu\text{m}$  pore size polycarbonate filter. Samples were removed to determine initial DOC concentrations and optical properties, and water was then dispensed into eighteen 60-ml glass biological oxygen demand (BOD) bottles per treatment.

BOD bottles were incubated in the dark while submerged in a recirculating water bath maintained at 20°C. At time zero and after 13, 27, 36, and 51 d of incubation, three of the replicate BOD bottles prepared from each treatment were sacrificed for determination of dissolved oxygen concentration using precision Winkler titrations with a Mettler DL-21 automatic titrator (Pomeroy et al. 1994). Formation of gas bubbles during extended incubations was prevented by warming sample water to 22°C and applying a light vacuum

prior to filling the bottles. At the final time point, additional BOD bottles were sacrificed for analysis of DOC concentration and measurement of optical properties.

**DOC analysis**—DOC concentrations were measured using a Shimadzu TOC-5000 carbon analyzer calibrated with potassium biphthalate. Duplicate samples were filtered through ashed Whatman GF/F filters and stored at 2°C. Samples were acidified to pH 3 with 10% phosphoric acid and sparged with CO<sub>2</sub>-free air for 15 min just prior to analysis. A minimum of five injections was made per sample.

**Optical measurements**—Absorbance scans over the wavelength range of 250–800 nm were performed on a Beckman DU-640 UV-visible scanning spectrophotometer using 1 cm (250–450 nm wavelength range) and 5 cm (355–800 nm wavelength range) cuvettes. Absorption coefficients were calculated as  $a_\lambda = 2.303 * A_\lambda / l$ , where  $a_\lambda$  is the absorption coefficient at wavelength  $\lambda$ ,  $A_\lambda$  is the absorbance at wavelength  $\lambda$ , and  $l$  is the path length of the quartz cuvette (in meters). Absorptivity at 350 nm (i.e.,  $a_{350}$ ) was used as the index of colored dissolved organic matter (CDOM) concentrations for most analyses. In some cases, absorptivity at a representative visible wavelength ( $a_{450}$ ) or integrated absorption between 250 nm and 500 nm (on the basis of trapezoidal integrations under the curve of absorption coefficient vs. wavelength) was used to represent CDOM concentrations.

Spectral slope coefficients were calculated by two methods. First, absorption coefficient data were linearized by log transformations, and spectral slopes were estimated from a least-squares linear regression of log absorptivity versus wavelength (Jerlov 1968). Second, absorption coefficient were fit to a nonlinear equation in the following form: absorptivity =  $A \exp[-S(\lambda - \lambda_0)]$ , where  $A$  is the absorptivity at  $\lambda_0$  (i.e., 290 nm) and  $S$  is the spectral slope coefficient (Zepp and Schlotzhauer 1981; Blough and Green 1995) using Sigma Stat (SPSS). Slopes were calculated over the spectral regions 290–400 nm (using data from the 1-cm cuvette) and 290–700 nm (using data from both 1-cm and 5-cm cuvettes combined by concatenating scans in the 380–420 nm range).

Samples for fluorescence excitation–emission matrices (EEMs) were diluted with Nanopure dH<sub>2</sub>O to the point where  $A_{350}$  was below 0.02 to minimize inner filtering effects. High-resolution fluorescence matrix scans were performed from 250–500 nm excitation (5-nm intervals) and 290–600 nm emission (2-nm intervals) using an ISA SPEX Fluorolog 3-12 scanning fluorometer with R928P detector. The instrument was configured for signal ratio mode and dark offset, and both excitation and emission slits were set to 5 nm bandpasses. Scans were corrected for instrument configuration according to the manufacturer's guidelines and Coble et al. (1993) and converted to quinine sulfate equivalents according to Coble et al. (1998). Rayleigh and Raman scatter peaks were eliminated during postprocessing of the data in Matlab (Release 11). An algorithm was developed to excise scatter peaks (i.e., peak emission  $\pm$  10–15 nm at each excitation wavelength) from the scan data and replace the excised values using three-dimensional interpolation of the remaining data (Delaunay triangulation method). The inter-

polated surface was constrained to pass through the nonexcised values so that only data in excised portions were interpolated. Following correction and scatter removal, the fluorescence from the Nanopure water diluent was subtracted from each scan and the fluorescence values were multiplied by the dilution factor to calculate the EEM for the original undiluted sample.

**Replication in a solar simulator**—The volumes of water needed for biological measurements necessitated the use of a large-scale fluorescent light bank for irradiations in the primary experiment. Since this light bank produced light of low intensity with mercury emission peaks, the experiment was replicated on a smaller scale using a Suntest CPS solar simulator with a high-pressure xenon lamp and special UV filter for sample irradiation. Light output from the Suntest instrument was 40 W m<sup>-2</sup> UVA, 1.4 W m<sup>-2</sup> UVB, and 380 W m<sup>-2</sup> PAR. This light output matched the natural solar spectrum at midafternoon in June at 30° latitude.

Water for the replication experiment was collected from the Satilla River estuary in November 1998; initial DOC concentration was 1971  $\mu$ M C. Water was placed in 160-ml quartz flasks with a 30-ml head space and irradiated in 50-min sessions, separated by 10-min cooling periods on ice to minimize sample heating; this process was repeated until target photobleaching levels were reached (up to 40 h of irradiation for the most photobleached treatment). Because of size limitations with the Suntest instrument, there was insufficient sample to conduct respiration measurements during the bioassay phase of the experiment, but all other experimental protocols (i.e., measurement of optical properties and carbon budgeting) were identical to those described for the primary experiment.

## Results

**Direct effects of photobleaching on DOM and CDOM**—Exposure of estuarine DOM to irradiation resulted in significant loss of absorptivity in UV and near-visible wavelengths (280–550 nm) (Fig. 1). Greatest losses of CDOM were centered at 350 nm and ranged from 15.9–63.8% (expressed as a percentage of the original  $a_{350}$  value), depending on the length of exposure (Table 1). In dark controls, the decrease in  $a_{350}$  was 1.6% (nonincubated dark control) and 4.0% (incubated dark control). CDOM losses at a representative visible light wavelength (450 nm) were less pronounced, ranging from 9.6–50.4%, depending on the length of exposure.

Decreases in DOC caused by direct photochemical mineralization amounted to 9.4–30.7% of the initial pool, depending on length of exposure (Fig. 2). DOC loss did not keep pace with absorptivity decreases (Table 1)—DOC losses were approximately 60% of those measured for  $a_{350}$  during the initial photobleaching stages but only 48% at longer irradiation times (Fig. 2). Results from the replication experiment were similar, and likewise showed that photochemically mediated DOC losses did not keep pace with absorptivity losses during extended photodegradation (Table 1).

**Effects of photobleaching on biological degradation**—Bacterial degradation of estuarine DOC from the Satilla Riv-

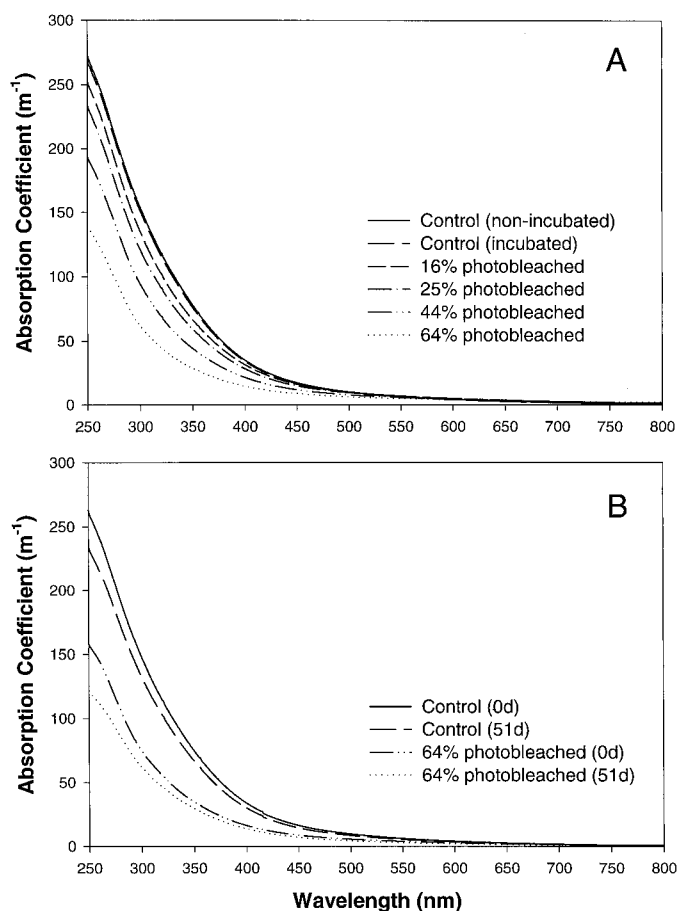


Fig. 1. Absorbance spectra of Satilla Estuary DOM (A) following varying levels of photobleaching and (B) before and after biological degradation of the nonincubated control and the 64% photobleached treatment. Spectra in B were measured after the addition of an inorganic nutrient solution and bacterial inoculum.

er in the absence of prior photochemical degradation occurred very slowly. Over a 51-d period, only 47  $\mu\text{M C}$  (nonincubated dark control) and 58  $\mu\text{M C}$  (incubated dark control) (2.5 and 2.9% of the DOC pool) was respired by the estuarine bacterial community, as estimated from  $\text{O}_2$  consumption and assuming a respiratory quotient of one. Kinetics of biological degradation were nearly linear over the 51-d period (Fig. 3). Furthermore, extended incubation of the nonincubated dark control showed linearity in biological degradation rates for up to 135 d (not shown). Such a low and constant rate of respiration over several months of incubation is consistent with the absence of a significant reservoir of labile, rapidly cycling DOC in the Satilla Estuary, probably reflecting the strong influence of watershed-derived organic matter of soil and vascular plant origin.

Exposure of DOC from the Satilla Estuary to simulated sunlight significantly increased subsequent rates of biological degradation. During the 51-d biological degradation phase, bacteria respired 110  $\mu\text{M C}$  (16% photobleached treatment) to 153  $\mu\text{M C}$  (64% photobleached treatment), as estimated from  $\text{O}_2$  consumption. When DOC losses were expressed on a percentage basis (to account for variations in

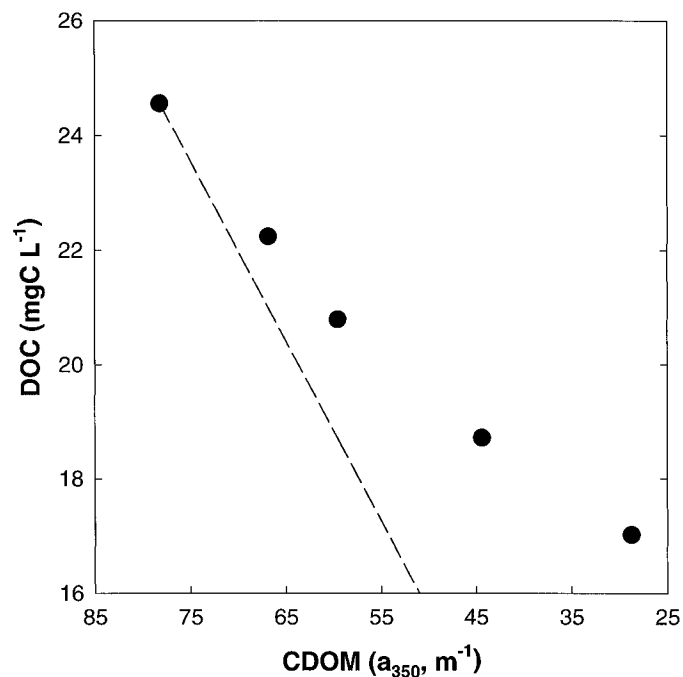


Fig. 2. DOC concentration plotted as a function of CDOM absorbance during extended photodegradation of Satilla Estuary DOM (primary experiment). CDOM was measured as absorptivity at 350 nm. The dotted line represents a theoretical 1 : 1 relationship between DOC and CDOM based on initial values. The replication experiment showed a similar relationship between DOC and CDOM (not shown). Confidence limits (95%) for the x- and y-axes are obscured by the data points.

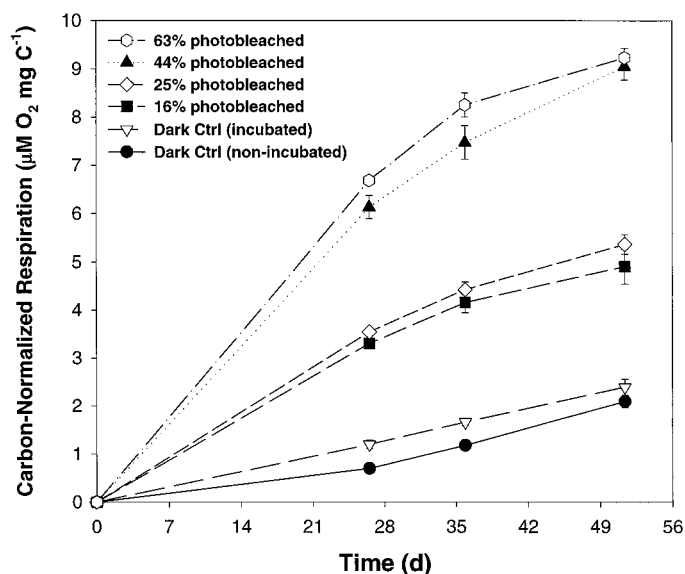


Fig. 3. Bacterial respiration of Satilla Estuary DOM during 51-d dark incubations (primary experiment) plotted as a function of the extent of prior photodegradation. Respiration losses were divided by initial DOC concentration to account for differences in starting concentrations between treatments. Error bars indicate the 95% confidence limits for three replicate samples calculated by the formula of Ott (1984) for difference calculations.

Table 2. Degradation of dissolved organic carbon (DOC) during the 51-d biological degradation phase following photobleaching. Changes ( $\Delta$ ) are expressed relative to postphotobleaching values and are calculated from measurements of bacterial respiration (i.e.,  $O_2$  consumption) or DOC concentrations. Sample volume constraints did not permit bacterial respiration measurements in the replication experiment.

Experiment/treatment	Initial DOC concentration $\mu\text{M}$ C $\pm$ 95%	$\Delta$ DOC (respiration-based)		$\Delta$ DOC (concentration-based)	
		$\mu\text{M}$ C $\pm$ 95%	%	$\mu\text{M}$ C $\pm$ 95%	%
Primary experiment					
Control (nonincubated)	1,886 $\pm$ 32	47 $\pm$ 3	-2.5	215 $\pm$ 22	-11.4
Control (incubated)	2,004 $\pm$ 19	58 $\pm$ 4	-2.9	209 $\pm$ 26	-10.4
16% photobleached	1,874 $\pm$ 27	110 $\pm$ 8	-5.9	261 $\pm$ 21	-13.9
25% photobleached	1,739 $\pm$ 28	112 $\pm$ 4	-6.4	261 $\pm$ 20	-15.0
44% photobleached	1,548 $\pm$ 21	168 $\pm$ 5	-10.9	292 $\pm$ 20	-18.9
64% photobleached	1,386 $\pm$ 16	154 $\pm$ 3	-11.1	322 $\pm$ 15	-23.3
Replication experiment					
Control (nonincubated)	1,946 $\pm$ 34	—	—	170 $\pm$ 50	-8.7
Control (incubated)	1,881 $\pm$ 43	—	—	171 $\pm$ 48	-9.1
12% photobleached	1,728 $\pm$ 32	—	—	227 $\pm$ 35	-13.1
21% photobleached	1,563 $\pm$ 22	—	—	177 $\pm$ 27	-11.3
32% photobleached	1,498 $\pm$ 27	—	—	170 $\pm$ 34	-11.3
59% photobleached	1,249 $\pm$ 21	—	—	194 $\pm$ 33	-15.5

DOC concentration at the end of the preceding photodegradation phase), the susceptibility of Satilla Estuary DOC to biological degradation increased as a function of the extent of prior photobleaching (Fig. 3). Biological degradation of DOC based on changes in DOC concentration, though a less sensitive measure in these experiments than respiration-based estimates, likewise showed that exposure to sunlight increased the susceptibility of the remaining DOC pool to biological degradation (Table 2). The solar simulator replication experiment showed similar trends in biological reactivity with progressive photobleaching (Table 2).

*Alterations to spectral slope coefficient*—Photodegradation of Satilla Estuary DOM modified the spectral slope (i.e., the absolute value of the slope of the plot of log absorptivity vs. wavelength) (Table 1). Spectral slopes in the primary experiment (calculated over the wavelength range of 290–400 nm using the nonlinear least-squares regression method; Zepp and Schlotzhauer 1981) ranged from 0.0141 (in the dark controls) to 0.0156 (in the 64% photobleached treatment) and increased with length of irradiation. Spectral slopes in the replication experiment ranged from 0.0146 (in the dark controls) to 0.0155 (in the 59% photobleached treatment), although the spectral slope did not substantially increase in this experiment until the samples were extensively photodegraded (59% photobleached treatment).

Bacterial degradation did not affect spectral slope in the dark controls, but decreased the absolute value of the spectral slopes (i.e., shifted slopes in the opposite direction to the photochemical shifts) for all photobleached treatments (Fig. 4). Following the 51-d biological degradation phase, spectral slopes ranged from 0.0141 (in the dark controls) to 0.0153 (in the 64% photobleached treatment).

Calculation of spectral slopes over a longer wavelength interval (290–700 nm), or using the more traditional linear least-squares fit to log-transformed data, gave similar results,

although the  $r^2$  values for the linear least-squares method (0.96 to 1.0) were slightly lower than for the nonlinear model (0.99 to 1.0). Results of the replication experiment likewise showed bacterially mediated decreases in spectral slope for DOM that had first been photodegraded (Fig. 4).

*Alterations to fluorescence properties*—Photodegradation of Satilla River DOM removed 56% of the original natural fluorescence in the 63% photobleached treatment. In contrast, loss of fluorescence during the biological degradation treatment phase was only 4% (Table 3).

We compared fluorescence intensity of four regions of the excitation–emission matrix, including a primary fluorescence peak from dissolved humic substances (peak A), a secondary humic-substances peak characteristic of terrestrially derived DOM (peak C), a secondary humic-substances peak characteristic of marine-derived DOM (peak M), and a peak attributable to fluorescence from aromatic amino acids, primarily tryptophan (peak T; Coble 1996; Mayer et al. 1999; see Fig. 5). C fluorophores were somewhat more susceptible to photochemical degradation than A and M fluorophores and total fluorescent dissolved organic matter (FDOM) (Table 3). An increase in amino acid fluorescence (peak T) was seen in dark controls, indicating that bacterial transformation of nonphotodegraded estuarine DOM can be a source of new fluorophores. T fluorophores also appeared to be less susceptible to photodegradation (Table 3). FDOM responses in the replication experiment were similar to those in the primary experiment.

*Relative DOM, CDOM, and FDOM degradation*—Changes in bulk DOC concentrations were compared to changes in CDOM (measured as integrated absorbance in the 250–500 nm wavelength range) and FDOM (measured as integrated fluorescence at excitation wavelengths from 250–500 nm). Bulk DOM was lost more slowly than was color or

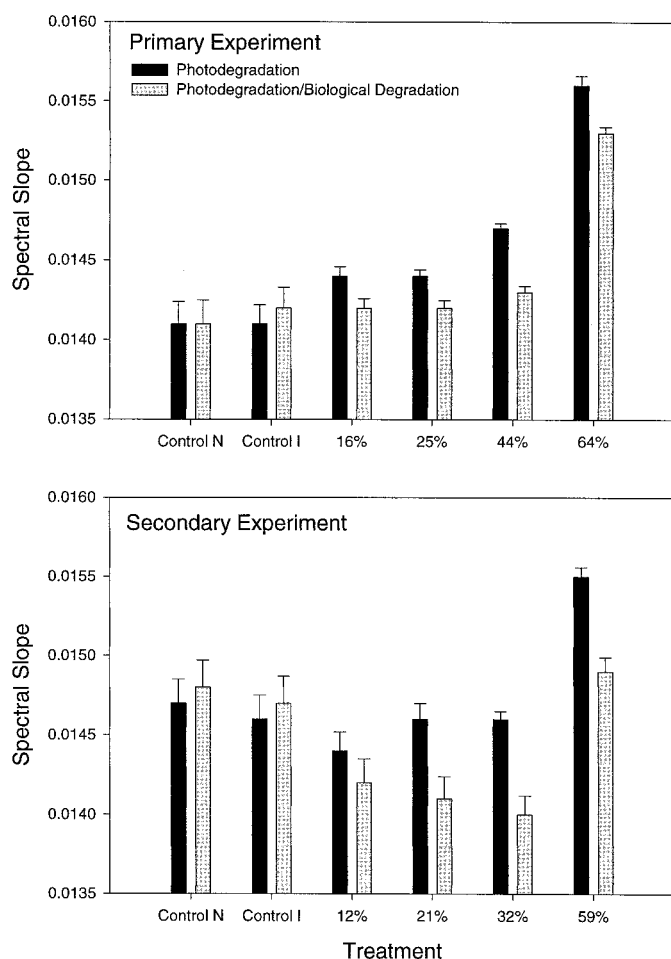


Fig. 4. Absolute values of the spectral slope coefficient,  $S$ , for Satilla Estuary DOM following photochemical and biological degradation. Postphotodegradation  $S$  values were calculated for samples that had been prepared for biological degradation (i.e., following addition of inoculum and nutrients) to allow direct comparison with postbiological degradation data; for this reason, the values may differ slightly from those in Table 1. All samples were filtered (0.2- $\mu\text{m}$  pore size) prior to optical analysis. Control  $N$  = nonincubated dark control. Control  $I$  = incubated dark control. Error bars represent the standard error for the estimate of  $S$ .

fluorescence during both photochemical and biological decomposition, with rates of DOM removal approximately 60% of the removal of CDOM and FDOM pools. FDOM losses outpaced CDOM losses during photobleaching, but were lower than CDOM losses during biological degradation (Table 3).

When CDOM and FDOM losses were expressed on a percentage basis (to account for differing pool sizes at the beginning of the biological degradation phase), the relative susceptibility of Satilla Estuary CDOM and FDOM to biological degradation increased after photobleaching. In the primary experiment, bacterial degradation of CDOM amounted to 19% of the pool that remained after long-term photobleaching (compared with 9.7% of the nonbleached pool); similarly, bacterial degradation removed 17% of the FDOM pool that remained after extended photobleaching

(compared with 4.4% of the nonbleached). The solar simulator replication experiment showed similar increases in biological reactivity of the material that remained after extended photobleaching (13% of the bleached CDOM vs. 5% of the nonbleached; 10% of the bleached FDOM vs. 0% for the nonbleached). Considering photochemical and biological losses together, 38% of the original DOM, 59% of the CDOM, and 63% of the FDOM was removed when extensive photodegradation was followed by long-term biological degradation (Table 3).

## Discussion

Our experimental results address two aspects of DOM photochemistry in coastal environments: 1) the potential role of photochemical processes in controlling the residence time of terrestrially derived DOM in the ocean, and 2) the influences of photochemical processes on terrestrially derived light-absorbing material resident in coastal systems.

*Terrestrial DOM in the ocean*—Although terrestrial DOM is expected to be highly resistant to biological degradation, current understanding of oceanic DOM pools and fluxes indicates that it has a shorter residence time in the ocean than does marine-derived (presumably more labile) DOM (Hedges 1992). Recent speculations on this problematic aspect of the global carbon budget have focused on photodegradation as a mechanism by which the residence time of terrestrially derived DOM in the ocean could be decreased, both through direct photochemical mineralization to dissolved inorganic carbon and  $\text{CO}$  (Miller and Zepp 1995; Amon and Benner 1996) and stimulation of biological mineralization (Kieber et al. 1989; Miller and Moran 1997). In this case, photochemical reactivity, rather than biological reactivity, would be the key factor controlling DOM residence time in seawater. Models assuming first-order photodegradation kinetics of terrestrial DOM in seawater predict half-lives as short as 1.5 yr for riverine DOM in the ocean mixed layer (Mopper et al. 1991; Miller and Zepp 1995). The accuracy of these models, however, ultimately depends on the time scales over which photochemically mediated DOM losses operate and the kinetics of the photodegradation process, both of which are poorly understood.

Our results provide evidence that a significant fraction of the terrestrially derived DOM pool can be photodegraded during extended exposure to low levels of sunlight. Significant losses of DOC (>30%), CDOM (>50%), and FDOM (>55%) occurred throughout long-term exposures of Satilla Estuary DOM to sunlight. Results of our laboratory studies concur with the direct field observations of Vodacek et al. (1997) of extensive photobleaching of terrestrially derived DOM on the continental shelf of the Middle Atlantic Bight and with the observations of Opsahl and Benner (1998) of rapid photodegradation of terrestrially derived lignin phenols in seawater.

Assessment of the importance of photodegradation as a mechanism for controlling turnover of terrestrial DOM in the ocean is complicated by a number of unresolved issues. First, evidence is accumulating that exposure to sunlight can in some cases decrease, rather than increase, subsequent

Table 3. Relative changes in carbon concentration, color, and fluorescence in Satilla Estuary dissolved organic matter (DOM) during long-term photobleaching and biological degradation. Changes ( $\Delta$ ) are expressed relative to the initial sample and are based on DOC concentrations (DOM), absorbance integrated from 250 to 500 nm (CDOM), and fluorescence integrated over the region defined by 250–500 nm excitation and 290–650 nm emission (FDOM). Fluorescence was also integrated over subsets of the excitation/emission matrix representing region A (defined as part of a circle centered at 150 nm Ex and 460 Em with a radius of 125 nm), region C (345 Ex, 460 Em, 25 nm radius), region M (312 Ex, 420 Em, 25 nm radius), and region T (275 Ex, 330 Em, 25 nm radius)(see Fig. 5). Ex/Em values indicate wavelength of excitation and emission for the fluorescence maximum in the combined C and M regions. Photo alone, only subjected to photobleaching; bio alone, only subjected to biological degradation (i.e., dark control); photo plus bio, sequential photobleaching and biological degradation.

Experiment/treatment	$\Delta$ DOM (%)	$\Delta$ CDOM (%)	$\Delta$ FDOM (%)	$\Delta$ FDOM regions (%)				Fluorescence maximum Ex/Em
				A	C	M	T	
Primary experiment								
initial								323/447
photo alone (64%)	-30.7	-49.5	-55.5	-53.7	-61.1	-52.7	-44.6	310/434
bio alone (51 d)	-2.9	-10.6	-4.4	-11.2	-12.2	-11.9	+112.0	320/445
photo plus bio	-38.4	-59.0	-62.9	-62.0	-66.9	-62.6	-55.3	313/439
Replication experiment								
initial								331/446
photo alone (59%)	-35.8	-52.9	-66.0	-61.5	-66.8	-56.4	-37.0	312/429
bio alone (51 d)	-9.1	-3.7	+0.2	+0.1	-0.5	-0.8	+22.5	331/452
photo plus bio	-45.8	-58.8	-69.3	-67.5	-70.6	-64.1	-24.6	315/430

rates of biological degradation of DOM in surface seawater (Benner and Biddanda 1998; Obernosterer et al. 1999), presumably because the photochemical formation of biologically refractory compounds outpaces the formation of biologically labile compounds. However, our experiments with terrestrial DOM from a southeastern U.S. estuary show consistently positive net effects on biological degradation, extending at least to the point where two-thirds of the photochemically reactive DOM has been removed. These results, combined with studies from marine and freshwater ecosystems that point to recently produced algal-derived DOM as the main target of inhibitory effects (Benner and Biddanda 1998; Tranvik and Kokalj 1998), suggest that the net effect of sunlight exposure on terrestrial (perhaps primarily vascular plant derived) DOM in estuaries and coastal oceans is to enhance its biological availability.

A second issue related to understanding the long-term effects of photodegradation on terrestrially derived DOM in the ocean is the presence of nonphotoreactive components of the DOM pool. Measures of lignin-derived phenols in Mississippi River water suggested a residual, nonphotoreactive fraction equivalent to 25% of the original material (Opsahl and Benner 1998). Likewise, studies of photochemical dissolved inorganic carbon formation in coastal seawater indicate that only 15% of the DOC pool is susceptible to direct mineralization during extensive photobleaching (Miller and Zepp 1995). We examined the Satilla Estuary results for evidence of a nonreactive component by fitting the data to two competing exponential decay models, one with a residual (nonreactive) component and one without. For losses of DOC directly mediated by photochemistry (i.e., photobleaching phase alone), a better fit was obtained with the residual model ( $r^2 = 0.98$  and  $0.96$  for the primary and replication experiments) than with the simple exponential model ( $r^2 = 0.88$  and  $0.84$ ). The difference between the models was statistically significant ( $F$  test discrimination among

competing models,  $P < 0.05$ ; Robinson 1985), with the residual model predicting a nonreactive component equal to 69% (primary experiment) and 65% (replication experiment) of the original DOC.

We repeated the curve-fitting exercise after including DOC losses caused by photochemically stimulated biological mineralization of DOC (i.e., the photoproducts that initially remain as part of the DOM pool but were subsequently mineralized by biological routes; Miller and Zepp 1995). This pool of labile DOM photoproducts was estimated as the enhanced bacterial respiration of DOC that occurred following photodegradation (during the 51-d biological phase). As before, the total loss of DOC (the sum of direct photochemical degradation plus photochemically enhanced biological degradation) was best modeled with a residual component ( $r^2 = 0.98$  and  $0.92$  for the primary and replication experiments) than without ( $r^2 = 0.89$  and  $0.82$ ), and the difference between the models was statistically significant ( $P < 0.01$ ) for the primary experiment.

The results of this curve-fitting exercise are not presented as an argument for the existence of a completely nonphotoreactive component of terrestrial DOC. The approach is limited by the small number of time points ( $n = 5$ ) that precludes a robust test of other, more parameter-rich models that may fit the data equally well or better (for example, the sum of exponentially degrading fast and slow components, or the sum of multiple linearly degrading components). Nonetheless, the results indicate that simple first-order models do not provide the best fit for long-term photodegradation of terrestrial carbon because the amount of sunlight required to bring about an equivalent proportional loss of the DOC pool increases as photodegradation progresses, even when delayed DOC mineralization that occurs via enhanced bacterial activity is considered. This pool of resistant DOC may represent components of the original material that are especially refractory to photochemical degradation, or it may

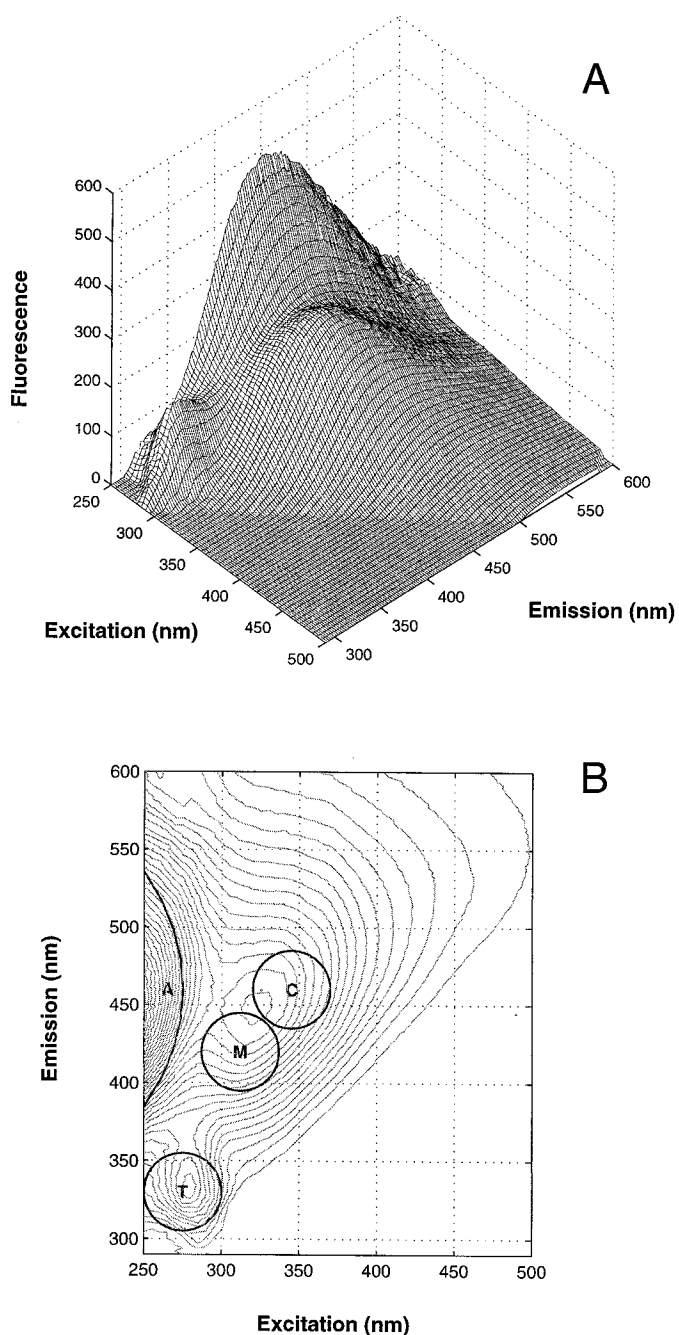


Fig. 5. Excitation/emission fluorescence matrix for Satilla Estuary DOM (initial sample; primary experiment) shown as (A) a three-dimensional plot and (B) a contour plot with locations of the four major fluorophore regions (Coble et al. 1996) indicated. Fluorescence is expressed in quinine sulfate equivalents.

represent the conversion of original material into photochemically refractory forms during exposure to sunlight (Benner and Biddanda 1998; Tranvik and Kokalj 1998; Obnerosterer et al. 1999). In either case, predictions based on first-order models are likely to overestimate the photochemical removal rate of terrestrial DOM from the ocean.

Similar model comparisons for CDOM bleaching, however, showed that the experimental data were adequately de-

scribed by a simple exponential decay model and that invoking a more complex residual model did not provide a statistically better fit. Thus CDOM bleaching and DOC removal may be uncoupled during long-term photodegradation of terrestrial material in the ocean. From a theoretical standpoint, a pure chromophore in an optically thick solution (i.e., a solution that absorbs all incident sunlight) would be expected to bleach linearly rather than exponentially (Zepp and Cline 1977), although a complex mixture of chromophores with varying rates of direct or sensitized photobleaching could produce an aggregate curve that is best fit by an exponential model (Zepp 1988).

*Light-absorbing DOM in coastal environments*—CDOM absorption typically dominates total UV absorption in seawater (DeGrandpre et al. 1996). In coastal environments, this dominance can extend into visible wavelengths (Nelson and Guarda 1995), and thus CDOM can compete with primary producers for photosynthetically available radiation, as well as contribute to error in satellite estimates of chlorophyll and primary production. In estuaries and coastal regions, CDOM exported from rivers and coastal marshes is the primary source of light-absorbing material, and thus its photochemical and biological degradation are critical determinants of the optical properties of the resident seawater.

The spectral slope parameter provides a mechanism for estimating CDOM absorptivity across the solar spectrum and comparing optical properties of CDOM over time and space (Zepp et al. 1998). The current lack of consistency in how spectral slopes are calculated (with regard to wavelength region and computation method) makes direct comparisons across studies problematic (Coble and Brophy 1994). Nonetheless, the spectral slopes computed in this study for Satilla River CDOM (0.0137 to 0.0156) are similar to those reported in other estuaries and coastal regions, including the continental shelf of the southeastern United States into which the Satilla River drains (0.0173; Nelson and Guarda 1995) and the Middle Atlantic Bight (0.014 to 0.020; Vodacek et al. 1997).

It has been suggested that both photochemical and biological processes can modify CDOM spectral slopes (Miller 1994; Vodacek et al. 1997). Our results show that photochemical degradation of terrestrial DOM generally causes an increase in the absolute value of the spectral slope, although this is most evident in extensively photodegraded CDOM. These results are in agreement with several field and laboratory studies (Vodacek et al. 1997; Del Vecchio, Vodacek and Blough in prep.), but not with all previous studies of DOM photodegradation (Miller 1994; Gao and Zepp 1998; Del Castillo et al. 1999). Previous work suggests that dissolved compounds of lower molecular weight (as might be expected to result from extended photodegradation) exhibit higher spectral slopes (Carder et al. 1989; Pages and Gadel 1990), but this trend is not consistent across all natural waters (Mopper et al. 1996).

Biological degradation did not affect the spectral slope when the CDOM had no prior history of photochemical degradation, indicating that the small amount of CDOM that could be removed by bacteria (Table 3) was removed relatively evenly across all wavelengths. These results concur

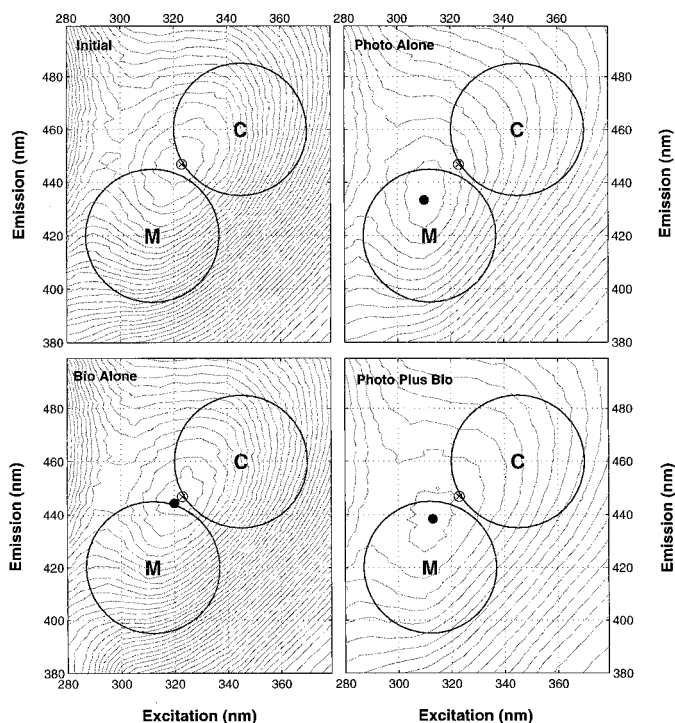


Fig. 6. Location of fluorescence excitation/emission maxima in the region of the C and M fluorophores for Satilla Estuary DOM for the nonincubated control (open circle), and following extensive photobleaching (64% photobleaching treatment), biological degradation (51-d biodegradation treatment), and sequential photobleaching and biological degradation (closed circles). The control maximum (open circle) is repeated on all panels. The replication experiment exhibited similar shifts in the location of the excitation/emission maxima (not shown). Contour lines are drawn at five quinine sulfate equivalent intervals.

with those of Pages and Gadel (1990). For DOM that had undergone photodegradation, however, consistent decreases in the absolute value of the spectral slope were evident (Fig. 4). Sequential photochemical and biological degradation of terrestrial CDOM therefore results in compensating effects on the spectral slope that dampen shifts occurring from photobleaching alone.

*Fate of FDOM during long-term photobleaching*—FDOM removal was slightly biased toward fluorophores attributed to terrestrially derived humic substances (C region fluorophores) on a percentage basis (Table 3), as well as in absolute units. Del Castillo et al. (1999) found decreases in wavelengths for the emission maxima of fluorophores in the C and M regions (treated as a combined H fluorophore) in the Orinoco River plume that they attributed to photodegradation. Our experiments likewise show that the excitation and emission maxima of these fluorophores decrease during photodegradation (Table 3), a shift that is the predicted result of preferential photobleaching of the C region fluorophores (Fig. 6). Bacterial degradation shifted the excitation/emission maxima in the opposite direction, although very slightly, for both photodegraded and nonphotodegraded material (Fig. 6). Thus as for spectral slope, we found that biological activity

slightly reversed the changes in DOM optical properties caused by photodegradation.

We saw significant photochemical degradation of A fluorophores (the primary fluorescence peak from dissolved humic substances) in Satilla River DOM, in contrast with field results from the Orinoco River plume suggesting that A fluorophores are not susceptible to photobleaching (Del Castillo et al. 1999). The most dynamic portion of the Satilla EEMs was the T region that has been previously attributed to fluorescence from aromatic amino acids (Coble 1996; Mayer et al. 1999). T region fluorophores were produced by bacteria from Satilla River DOM and were less susceptible to photodegradation than the humic substances fluorophores. Thus these fluorophores may be an indication of recent bacterial decomposition activity, at least for DOM of estuarine or terrestrial origin.

*A vascular plant-influenced end member*—The Satilla River delivers  $47 \times 10^3$  t of terrestrially derived DOC to the coastal ocean of the southeastern United States each year, about 60% of which is operationally defined as humic substances. This material is both highly colored (mean  $a_{350}$  values of  $72 \text{ m}^{-1}$  for six sample dates from December 1997 through March 1999) and highly fluorescent (mean fluorescence at Ex 360/Em >450 nm of 595 quinine sulfate units), and the temporal variation in color and fluorescence is large (up to threefold among our six sample dates). As may be typical of blackwater systems, the Satilla River represents a vascular plant-derived end member for estuarine DOM, characterized by an abundance of organic matter chemically similar to soil fulvic acids (Beck et al. 1974) and by a shortage of recent algal-derived organic matter. In keeping with these characteristics, Satilla River DOM had the highest aromaticity in an intercomparison of several U.S. estuaries (Hopkinson et al. 1998), whereas the biological lability of Satilla Estuary DOC (only 2–3% of the DOC pool; Table 2) was significantly lower than the U.S. estuaries (Hopkinson et al. 1998) and the worldwide riverine average (19% of the DOC pool; Søndergaard and Middelboe 1995).

Our studies of this vascular plant-influenced end member indicate that photochemical processes efficiently remove carbon, colored components, and fluorescent components from the DOM pool and that these losses are mediated either by long periods of low-intensity irradiation or short periods of high-intensity irradiation. Biological removal of DOM, CDOM, and FDOM is consistently stimulated by prior photobleaching, even for extensively photodegraded material, and biological activity partially reverses changes in optical properties due to photobleaching. Whereas the results for this estuarine system are consistent and repeatable, there is little comparative information available for estuarine DOM that is lower in vascular plant and soil influences and higher in contributions from younger (recently produced) or algal-derived organic matter. Current understanding of the fate of terrestrially derived DOM in the ocean will directly benefit from comparative studies of diverse sources of terrestrial DOM to the coastal ocean.

## References

- AMON, R. M. W., AND R. BENNER. 1996. Photochemical and microbial consumption of dissolved organic carbon and dissolved

- oxygen in the Amazon River system. *Geochim. Cosmochim. Acta* **60**: 1783–1792.
- BECK, K. C., J. H. REUTER, AND E. M. PERDUE. 1974. Organic and inorganic geochemistry of some coastal plain rivers of the southeastern United States. *Geochim. Cosmochim. Acta* **38**: 341–364.
- BENNER, R., AND B. BIDDANDA. 1998. Photochemical transformations of surface and deep marine dissolved organic matter: Effects on bacterial growth. *Limnol. Oceanogr.* **43**: 1373–1378.
- BLOUGH, N. V., AND S. A. GREEN. 1995. Spectroscopic characterization and remote sensing of nonliving organic matter. p. 23–45 *In* R. G. Zepp and C. Sonntag [eds.], *Role of nonliving organic matter in the earth's carbon cycle*. Wiley.
- BUSHAW, K. L., AND OTHERS. 1996. Photochemical release of biologically available nitrogen from dissolved organic matter. *Nature* **381**: 404–407.
- CARDER, K. L., R. G. STEWARD, G. R. HARVEY, P. B. ORTNER. 1989. Marine humic and fulvic acids: Their effects on remote sensing of ocean chlorophyll. *Limnol. Oceanogr.* **34**: 68–81.
- CERRIER, J., J. E. BAUER, E. R. M. DRUFFEL, R. B. COFFIN, AND J. P. CHANTON. 1999. Radiocarbon in marine bacteria: Evidence for the ages of assimilated carbon. *Limnol. Oceanogr.* **44**: 730–736.
- COBLE, P. 1996. Characterization of marine and terrestrial DOM in seawater using excitation–emission matrix spectroscopy. *Mar. Chem.* **51**: 325–346.
- , AND M. M. BROPHY. 1994. Investigation of the geochemistry of dissolved organic matter in coastal waters using optical properties. *SPIE Vol. 2258 Ocean Optics* **12**: 377–389.
- , C. E. DEL CASTILLO, AND B. AVRIL. 1998. Distribution and optical properties of CDOM in the Arabian Sea during the 1995 southwest monsoon. *Deep-Sea Res. Part II Top. Stud. Oceanogr.* **45**: 2195–2223.
- , C. A. SCHULTZ, AND K. MOPPER. 1993. Fluorescence contouring analysis of DOC intercalibration experiment samples: A comparison of techniques. *Mar. Chem.* **41**: 173–178.
- DEGRANDPRE, M. D., A. VODACEK, R. K. NESLON, E. J. BRUCE, AND N. V. BLOUGH. 1996. Seasonal seawater optical properties of the U.S. Middle Atlantic Bight. *J. Geophys. Res.* **101**: 22,722–22,736.
- DEL CASTILLO, C. E., P. G. COBLE, J. M. MORELL, J. M. LÓPEZ, AND J. E. CORREDOR. 1999. Analysis of the optical properties of the Orinoco River plume by absorption and fluorescence spectroscopy. *Mar. Chem.* **66**: 35–51.
- GAO, H., AND R. G. ZEPP. 1998. Factors influencing photoreactions of dissolved organic matter in a coastal river of the southeastern United States. *Environ. Sci. Technol.* **32**: 2940–2946.
- HEDGES, J. I. 1992. Global biogeochemical cycles: Progress and problems. *Mar. Chem.* **39**: 67–93.
- HERNDL, G. J., A. BRUGGER, S. HAGER, E. KAISER, I. OBERNOSTERER, B. REITNER, AND D. SLEZAK. 1997. Role of ultraviolet-B radiation on bacterioplankton and the availability of dissolved organic matter. *Plant Ecol.* **128**: 42–51.
- HOPKINSON, C. S., AND OTHERS. 1998. Terrestrial inputs of organic matter to coastal ecosystems: An intercomparison of chemical characteristics and bioavailability. *Biogeochemistry* **43**: 211–234.
- JEFFREY, W. H., J. P. KASE, AND S. W. WILHELM. 1999. Ultraviolet radiation effects on bacterioplankton and viruses in marine ecosystems. *In* S. J. deMora, S. Demers, and M. Vernet, [eds.], *The effects of UV radiation in the marine environment*. Cambridge Univ. Press.
- JERLOV, N. G. 1968. *Optical oceanography*. Elsevier.
- KIEBER, D. J., J. MCDANIEL, AND K. MOPPER. 1989. Photochemical source of biological substrates in sea water: Implications for carbon cycling. *Nature* **341**: 637–639.
- MAYER, L. M., L. L. SCHICK, AND T. C. LODER. 1999. Dissolved protein fluorescence in two Maine estuaries. *Mar. Chem.* **64**: 171–179.
- MILLER, W. L. 1994. Recent advances in the photochemistry of natural dissolved organic matter. p. 111–128 *In* G. R. Helz, and others [eds.], *Aquatic and surface photochemistry*. CRC Press.
- , AND M. A. MORAN. 1997. Interaction of photochemical and microbial processes in the degradation of refractory dissolved organic matter from a coastal marine environment. *Limnol. Oceanogr.* **42**: 1317–1324.
- , AND R. G. ZEPP. 1995. Photochemical production of dissolved inorganic carbon from terrestrial organic matter: Significance to the oceanic organic carbon cycle. *Geophys. Res. Lett.* **22**: 417–420.
- MOPPER, K., X. ZHOU, R. J. KIEBER, D. J. KIEBER, R. J. SIKORSKI, AND R. D. JONES. 1991. Photochemical degradation of dissolved organic carbon and its impact on the oceanic carbon cycle. *Nature* **353**: 60–62.
- , Z. FENG, S. B. BENTJEN, AND R. F. CHEN. 1996. Effects of cross-flow filtration on the absorption and fluorescence properties of seawater. *Mar. Chem.* **55**: 53–74.
- MORAN, M. A., AND R. G. ZEPP. 1997. Role of photoreactions in the formation of biologically labile compounds from dissolved organic matter. *Limnol. Oceanogr.* **42**: 1307–1316.
- , AND R. G. ZEPP. 2000. UV radiation effects on microbes and microbial processes. p. 201–228 *In* D. L. Kirchman and R. Mitchell [eds.], *Microbial ecology of the oceans*. Wiley.
- NELSON, J. R., AND S. GUARDA. 1995. Particulate and dissolved spectral absorption on the continental shelf of the southeastern United States. *J. Geophys. Res.* **100**: 8715–8732.
- OBERNOSTERER, I., B. REITNER, AND G. J. HERNDL. 1999. Contrasting effects of solar radiation on dissolved organic matter and its bioavailability to marine bacterioplankton. *Limnol. Oceanogr.* **44**: 1645–1654.
- OPSAHL, S., AND R. BENNER. 1998. Photochemical reactivity of dissolved lignin in river and ocean waters. *Limnol. Oceanogr.* **43**: 1297–1304.
- OTT, L. 1984. *An introduction to statistical methods and data analysis*. Second edition. Duxbury.
- PAGES, J., AND F. GADEL. 1990. Dissolved organic matter and UV absorption in a tropical hypersaline estuary. *Sci. Tot. Environ.* **99**: 173–204.
- POMEROY, L. R., J. E. SHELDON, AND W. M. SHELDON. 1994. Changes in bacterial numbers and leucine assimilation during estimations of microbial respiratory rates in seawater by the precision Winkler method. *Appl. Environ. Microbiol.* **60**: 328–332.
- ROBINSON, J. A. 1985. Determining microbial kinetic parameters using nonlinear regression analysis, p. 61–114. *In* K. C. Marshall [ed.], *Advances in microbial ecology*. Plenum.
- SØNDERGAARD, M., AND M. MIDDELBOE. 1995. A cross-system analysis of labile dissolved organic carbon. *Mar. Ecol. Prog. Ser.* **118**: 283–294.
- TRANVIK, L., AND S. KOKALJ. 1998. Decreased biodegradability of algal DOC due to interactive effects of UV radiation and humic matter. *Aquat. Microb. Ecol.* **14**: 301–307.
- VODACEK, A., N. A. BLOUGH, M. D. DEGRANDPRE, E. T. PELTZER, AND R. K. NELSON. 1997. Seasonal variation of CDOM and DOC in the Middle Atlantic Bight: Terrestrial inputs and photooxidation. *Limnol. Oceanogr.* **42**: 674–686.
- ZEPP, R. G. 1988. Environmental photoprocesses involving natural organic matter. p. 193–214 *In* F. H. Frimmel and R. F. Christman [eds.], *Humic substances and their role in the environment*. Wiley.
- , T. V. CALLAGHAN, AND D. J. ERICKSON. 1998. Effects of

- enhanced solar ultraviolet radiation on biogeochemical cycles. *J. Photochem. Photobiol. B Biol.* **46**: 69–82.
- , AND D. M. CLINE. 1977. Rates of direct photolysis in aquatic environment. *Environ. Sci. Technol.* **11**: 359–366.
- , AND P. F. SCHLOTZHAUER. 1981. Comparison of photochemical behavior of various humic substances in water: III. Spectroscopic properties of humic substances. *Chemosphere* **10**: 479–486.

*Received: 6 December 1999*

*Accepted: 24 April 2000*

*Amended: 15 May 2000*